Annals of Botany **125**: 485–494, 2020
doi: 10.1093/aob/mcz185, available online at www.academic.oup.com/aob

ANNALS OF BOTANY
Founded 1887

Photosynthetic cyclic electron transport provides ATP for homeostasis during trap closure in *Dionaea muscipula*

Daniel Maurer[1,*,†], Daniel Weber[2,†], Eva Ballering[1,3], Salah Alfarraj[4], Gada Albasher[4], Rainer Hedrich[5], Christiane Werner[3] and Heinz Rennenberg[1,4]

[1]Chair of Tree Physiology, Institute of Forest Sciences, University of Freiburg, Georges-Köhler-Allee 53/54, D-79110 Freiburg, Germany, [2]Phytoprove Plant Analytics UG, Senckenberg Biodiversity & Climate Research Centre, Georg-Voigt-Str. 14–16, D-60325 Frankfurt am Main, Germany, [3]Chair of Ecosystem Physiology, Institute of Forest Sciences, University of Freiburg, Georges-Köhler-Allee 53/54, D-79110 Freiburg, Germany, [4]College of Sciences, King Saud University, PO Box 2455, Riyadh 11451, Saudi Arabia and [5]Institute for Molecular Plant Physiology and Biophysics, Biocenter, University of Würzburg, D-97082 Würzburg, Germany

**For correspondence. E-mail daniel.maurer@ctp.uni-freiburg.de*

[†]These authors contributed equally to this work.

Received: 8 August 2019 Returned for revision: 15 October 2019 Editorial decision: 5 November 2019 Accepted: 8 November 2019
Published electronically 10 November 2019

• **Background and Aims** The processes connected with prey capture and the early consumption of prey by carnivorous *Dionaea muscipula* require high amounts of energy. The aim of the present study was to identify processes involved in flytrap energy provision and ATP homeostasis under these conditions.
• **Methods** We determined photosynthetic CO_2 uptake and chlorophyll fluorescence as well as the dynamics of ATP contents in the snap traps upon closure with and without prey.
• **Key Results** The results indicate that upon prey capture, a transient switch from linear to cyclic electron transport mediates a support of ATP homeostasis. Beyond 4 h after prey capture, prey resources contribute to the traps' ATP pool and, 24 h after prey capture, export of prey-derived resources to other plant organs may become preferential and causes a decline in ATP contents.
• **Conclusions** Apparently, the energy demand of the flytrap for prey digestion and nutrient mining builds on both internal and prey-derived resources.

Key words: ATP homeostasis, chlorophyll *a* fluorescence, *Dionaea muscipula* (Venus flytrap), electron transport, plant carnivory, photosynthesis, respiration.

INTRODUCTION

The Venus flytrap (*Dionaea muscipula*) grows natively in the swamp lands of North and South Carolina. This natural habitat is sunny and moist, but limited in soil-derived nutrients for plant growth and development (Roberts and Oosting, 1958; Brewer *et al.*, 2011). However, occasional fires lead to short periods with increased nitrogen (N) availability (Adamec, 1997; Schulze *et al.*, 2001; Ellison, 2006). In the course of evolution, these unfavourable conditions for nutrient acquisition by the roots led to the transformation of leaves to active capture organs in *D. muscipula* (Adlassnig *et al.*, 2005). Thereby leaves adapted functions of the roots (Bemm *et al.*, 2016; Hedrich and Neher, 2018). Traps were equipped to take up and store nutrients from captured prey (Kruse *et al.*, 2017) and even act as carbon sinks for organic carbon acquired from the roots (Gao *et al.*, 2015). As a consequence of the leaf taking over root functions, *D. muscipula* developed a reduced root system with 4–8 unbranched roots (Smith, 1931). Still *Dionaea* roots show surprisingly large constituent N uptake capacities, probably an adaption to irregular nutrient availability in the soil upon natural fires (Roberts and Oosting, 1958; Gao *et al.*, 2015). These adaptations helped *Dionaea* to overcome limitations by the nutrient-poor soil and provided advantages over non-carnivorous plants (Ellison, 2006; Kruse *et al.*, 2014).

Also in other plant species, leaves took over the functions of the roots. For example, Bromeliaceae developed leaf trichomes, which are able to absorb water and nutrients (Benzing, 2000). Tank-type, epiphytic Bromeliaceae grow in the canopy of tropical trees under nutrient-poor conditions (Lasso and Ackerman, 2013) and use detritus, which is falling into their tanks, for mineral nutrition. There are also some proto-carnivorous bromeliads which are able to use spider faeces or insects as an additional N source (Nishi *et al.*, 2013). Due to only occasional nutrient input, nutrients are taken up quickly, while excess N is stored in the form of amino acids in the leaves to support future plant growth and development (Benzing *et al.*, 1976; Takahashi and Mercier, 2011). Similarly, *Dionaea* quickly digests its prey, thereby providing N for immediate use, and stores excess N for future needs (Kruse *et al.*, 2017). In addition, during and after prey capture, *D. muscipula* reduce carbon autotrophy through photosynthetic CO_2 fixation (Pavlovič *et al.*, 2010; Kruse *et al.*, 2014) and use prey as an additional energy source through respiratory amino acid degradation

(Fasbender *et al.*, 2017). The rates of photosynthesis of *Dionaea* snap traps are not only low during prey capture and digestion, but in general are weak compared with non-carnivorous plant species (Bruzzese *et al.*, 2010; Ellison and Adamec, 2011).

This is also observed for mycoheterotrophs (Graham *et al.*, 2017) and hemiparasitic mistletoes that gain amino compounds (Escher *et al.*, 2004*a*) and carbohydrates (Escher *et al.*, 2004*b*) from the xylem sap of the host and, consequently, downregulate photosynthetic CO_2 fixation of their leaves. These changes of photosynthetic activity result in degraded plastomes with decreasing dependence on photosynthesis (Petersen *et al.*, 2015; Shin and Lee, 2018). Similar patterns were seen in carnivorous Lentibulariaceae (Wicke *et al.*, 2014), Droseraceae and *D. muscipula* (Nevill *et al.*, 2019). On the other hand, low photosynthetic rates of the traps of *Dionaea* constitute a trade-off between general photosynthetic activity required in addition to carbohydrate acquisition from prey and the use of photosynthetic carbon and energy for nutrient acquisition from prey capture (Ellison and Adamec, 2011). The functional changes of *Dionaea* traps upon prey capture are accompanied by changes in energy requirements. Touching trigger hairs of the Venus flytrap's leaf generates electrical signals (action potentials), which require energy (Volkov *et al.*, 2008). After an insect elicits two action potentials within 20 s, the trap closes within a fraction of a second (Escalante-Pérez *et al.*, 2014), resulting in high ATP consumption (Jaffe, 1973) with the H^+ ATPase upregulated to repolarize the trap membrane potential after depolarization following trigger hair mechanical stimulation (Hedrich and Neher, 2018). Considerable amounts of energy are subsequently required for expression of hydrolases (Bemm *et al.*, 2016; Scherzer *et al.*, 2017) and transporters (Scherzer *et al.*, 2013, 2015; Böhm *et al.*, 2016) as well as prey digestion plus mineral nutrient and carbohydrate acquisition from prey (Kruse *et al.*, 2014,; 2017; Fasbender *et al.*, 2017). Finally, energy is required to open the trap and to obtain turgor pressure and hydrodynamic flow for subsequent trap closure (Volkov *et al.*, 2012).

In the present study, we aimed to elucidate the role of photosynthesis for energy production upon closure of the snap traps and the early phase of prey consumption. In order to show energy production in the immediate response to trap closure, we simultaneously measured *in vivo* photosynthetic electron transport. Photosystem II (PSII) electron transport was monitored via fast fluorescence rise kinetics of prompt chlorophyll (Chl) *a* fluorescence (PF) and that of PSI via modulated 820 nm reflection (MR). Reflection changes at 820 nm provide information of the redox states of plastocyanin and P700. In addition, we monitored photosynthetic CO_2 uptake and changes in energy/ATP contents in response to trap closure. We hypothesized that *D. muscipula* switches from linear to cyclic electron transport as a strategy of additional energy production to increase ATP formation and to maintain energy homeostasis. The expression and upregulation of transporters and the transport of prey-derived resources itself are energy-intensive processes which consume ATP. Therefore, we hypothesized that ATP contents differ particularly in the midribs of fed and unfed traps. We further hypothesized that transiently prey-derived energy also supports ATP homeostasis of the traps.

MATERIALS AND METHODS

Plant material and the feeding experiment

Dionaea muscipula Ellis plants were obtained from a commercial supplier, raised in a glasshouse at 24 ± 4 °C and nourished with a slow-release fertilizer. After 3–4 months, plants were transferred to 350 cm^3 plastic pots containing nutrient-poor peat substrate. During experiments, *Dionaea* plants were grown in controlled-climate chambers with day/night cycles of 16/8 h, at 23/16 °C, 65 % relative humidity and 150 µmol photons m^{-2} s^{-1}. For feeding, traps were supplied with 10 mg of insect paste together with 25 µL of glutamine (Gln) solution (0.04 mg $µL^{-1}$) as previously reported (Kruse *et al.*, 2014; Fasbender *et al.*, 2017). For this purpose, the Gln solution was pipetted onto a round piece of cellulose filter of 6 mm in diameter (Schleicher & Schuell GmbH, Dassel, Germany), which was covered with the insect paste. Trichome hairs in the traps were stimulated mechanically for 10 s (at least ten touches) either without feeding or after the cellulose filter with the Gln solution and the insect paste was placed inside the trap. Similar sized traps with a length of about 25 mm were used for analysis.

Gas exchange and chlorophyll fluorescence measurements

For simultaneous gas exchange and Chl fluorescence measurements, traps were analysed using a portable gas exchange measuring system GFS-3000 (Heinz Walz GmbH, Effeltrich, Germany) equipped with an LED-Array/PAM Fluorometer 3033-FL clamped on the standard measuring head (Heinz Walz GmbH) with an 8 cm^2 cuvette window area. Before each measurement, traps were dark adapted for 30 min and dark respiration as well as dark-adapted maximum quantum yield of PSII (F_v/F_m) were determined. The standard conditions for gas exchange measurements in the cuvette were: trap temperature of 25 °C, saturating irradiance of 1500 µmol photons m^{-2} s^{-1} phosynthetically active radiation (PAR), CO_2 concentration of 400 µL L^{-1} and relative air humidity of 65 %. Traps were kept for 60 min in the light in the cuvette until CO_2 and H_2O vapour levels stabilized before traps were mechanically triggered with a fine wire for closure. Gas exchange measurements (data recorded every 2 s) and Chl fluorescence measurements (data recorded every 10 s) continued for 20 min. The effective quantum yield of PSII (Φ_{PSII}) and non-photochemical quenching (NPQ) were determined. The response time for gas exchange measurements has been adapted to Chl *a* fluorescence measurements. For calculation of gas exchange rates, projected trap areas were determined using graph paper and the Image software ImageJ (Schneider *et al.*, 2012).

Simultaneous measurements of the kinetics of prompt Chl a fluorescence (PF) and modulated 820 nm reflection (MR)

Prompt Chl *a* fluorescence (PF) measurements were conducted by reflective measurements on the outer surface of dark-adapted (20 min) traps (n = 8) with am M-PEA2 fluorimeter (Hansatech Instruments Ltd, King's Lynn, UK). A new battery-powered version of the 'Multifunctional Plant

Efficiency Analyser' (M-PEA2) was used for simultaneous measurements of PF and modulated 820 nm reflection (MR). The emitter wavelength of a non-modulated light source is 625 nm for the actinic light LED and 820 nm for the modulated light LED (light source for the modulated reflection). High-quality optical band pass filters are used for the detectors (PF 730 ± 15 nm, and reflection changes at 820 ± 20 nm). Measurements were performed on circular areas of the traps of 2 mm diameter, using Hansatech leaf clips homogeneously illuminated by actinic light LEDs set to a saturating light intensity of 3500 µmol photons m^{-2} s^{-1}. The detection of PF was recorded within seven different time intervals; every 10 µs for the initial fluorescence (0–300 µs), every 100 µs (0.3–3 ms), 1 ms (–30 ms), 10 ms (0.03–0.3 s), 100 ms (0.3–3 s), 1 s (3–30 s) and every 10 s (30–300 s). Raw data were transferred and processed using M-PEA Plus software (Hansatech Instruments Ltd). Chl *a* fluorescence induction curves (PF) were normalized to F_0 = 50 µs. Reflection values of a pulse-modulated light beam (modulated 820 nm reflection; MR) recorded simultaneously with the PF, were normalized to MR_0 at 0.7 ms expressed as MR/MR_0 (Strasser *et al.*, 2010; Chen *et al.*, 2016; Oukarroum *et al.*, 2016) using the open source software 'Libre Office 6' (The Document Foundation, Berlin, Germany). The data were plotted graphically by using 'Prism 8 for Mac OS-X' software (GraphPad Software Inc., La Jolla, CA, USA).

ATP measurement

ATP content was analysed in complete traps and in cut-out midribs of the traps. *Dionaea* traps were snap-frozen in liquid N, before midribs were cut out with a scalpel. Complete traps and frozen midribs were homogenized into powder with a mortar and pestle. ATP was extracted as described by Yang *et al.* (2002). Briefly, 20 mg of the frozen plant material were treated with 1 mL of distilled water, which was immediately heated in a boiling water bath for 10 min (Li *et al.*, 2017). The boiled lysates were centrifuged at 15 000 *g* for 5 min at 4 °C and the supernatants were collected for ATP measurements using an ATP assay kit (Calbiochem® Luciferase Luminescence ATP Assay Kit 119107-1KIT) following the manufacturer's protocol (Luminometer: TriStar² LB 942, Berthold Technologies GmbH & Co. KG, Bad Wildbad, Germany). *Dionaea* plants were kept in circadian rhythm (day/night cycles of 16/8 h) for ATP measurements 24, 48 and 72 h after trap closure.

Statistics

'Prism 8 for Mac OS-X' software (GraphPad Software Inc.) was used to determine significant differences of light intensities reflected in the near infrared at 820 nm (MR), as a probe for PSI activities. For this purpose, Brown–Forsythe and Welch one-way analysis of variance (ANOVA) tests (P = 0.05) were performed. Multi-comparison analyses were performed using the Dunnett's T3 test. The same statistical methods were used for analysing Chl *a* fluorescence induction curves (PF).

One-way ANOVA (P = 0.05, a = 0.95, Tukey's post-hoc test) was used to determine significant differences of ATP contents at different time points. Normal distribution of the data was tested using the Shapiro–Wilk test, and the homogeneity of variances was tested operating the Levene² test (both P = 0.05). The software ORIGIN PRO 2019 (OriginLab Corp., Northampton, MA, USA) was used for statistical analyses of ATP contents.

RESULTS AND DISCUSSION

Carbon assimilation and non-photochemical quenching

Trap closure upon consecutive mechanical stimulation of trigger hairs resulted in an immediate and rapid decrease in carbon assimilation (A) in fed and non-fed traps, with a minimum of –1.29 ± 0.71 µmol CO_2 m^{-2} s^{-1} (Fig. 1). This decrease was transient and carbon assimilation started to increase again already 30 s after trap closure. It largely recovered within the first 20 min after triggering, with carbon assimilation values of 1.50 ± 0.40 µmol CO_2 m^{-2} s^{-1}, but still was slightly lower than the initial carbon assimilation level of 1.75 ± 0.45 µmol CO_2

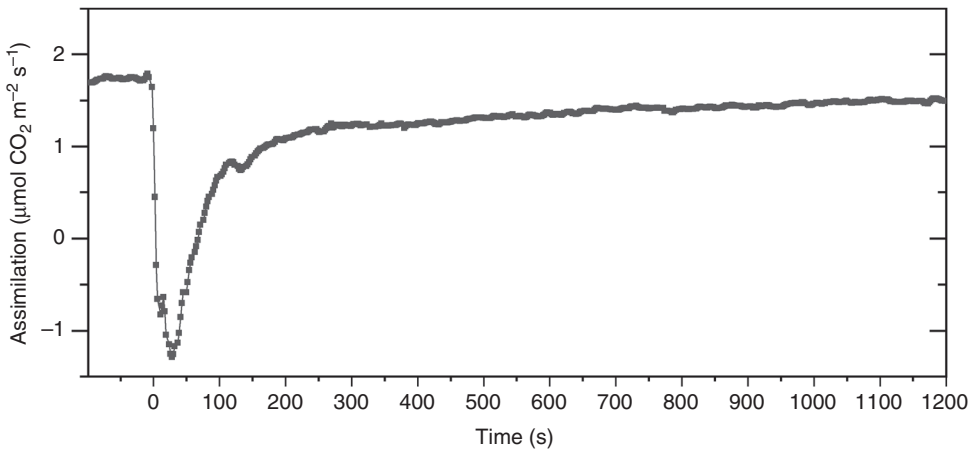

FIG. 1. Response of carbon assimilation in *Dionaea muscipula* after stimulation of trigger hairs (t = 0) (trap temperature 25 °C, light intensity 1500 µmol m^{-2} s^{-1} PAR, CO_2 concentration 400 µL L^{-1}, relative air humidity 65 %). Measurements were conducted using the portable gas exchange measuring system GFS-3000 equipped with an integrated PAM Fluorometer 3033-FL-Module (Walz). Data shown are mean values based on 12 independent measurements of both fed and non-fed traps (no significant differences between fed and non-fed traps).

m^{-2} s^{-1}. Carbon assimilation did not change significantly during the subsequent 24 h (data not shown).

Similar to the carbon assimilation, the effective quantum yield of PSII (Φ_{PSII}) showed a rapid, but transient decline upon closure of fed and non-fed traps. However, recovery was slow compared with carbon assimilation (Fig. 2). As observed for carbon assimilation, 20 min after trap closure the effective quantum yield was largely recovered, but was still slightly lower than initial pre-triggering values. At the same time, NPQ increased constantly, with the highest values 200 s after trap stimulation. Passing a maximum, NPQ decreased slowly, but was still significantly increased 20 min after trap closure compared with the pre-stimulation phase. Previous studies performed with cut *Dionaea* leaves revealed a similar rapid decrease of assimilation, but the recovery started already about 10 s after stimulation of the trigger hairs and trap closure (Pavlovič *et al*., 2010, 2011). Compared with previous studies, Φ_{PSII} decreased and recovered in a similar pattern (Pavlovič *et al*., 2010, 2011). In contrast, values of NPQ increased a lot faster and showed the highest values already 50 s after stimulation. Compared with this study, NPQ also decreased a lot quicker after its peak in previous investigations (Pavlovič *et al.*, 2011). However, as for carbon assimilation, previous studies used cut leaves for NPQ and Φ_{PSII} analyses rather than intact plants.

Modulated reflection

To elucidate whether these changes in photosynthetic carbon assimilation and electron transport are mediated by a transient switch from linear to cyclic electron transport, a deeper insight into the physiological state of the photosynthetic electron transport chain was necessary, since the information provided by calculating PSII fluorescence parameters solely based on two different measuring points (basal fluorescence F_0 and maximum fluorescence F_m) is limited. In cyclic electron transport, PSI plays a key role (Yamori *et al.*, 2016). Changes in the redox state of the PSI reaction centres (P700) and plastocyanin (PC) were monitored by measurements of modulated reflection (MR) at 820 nm, a well-established method to monitor PSI activity (Schreiber *et al.*, 1988; Klughammer and Schreiber, 1998). This parameter provides information about electron transport in the photosynthetic electron transport chain between PSII and PSI (Schansker *et al.*, 2003; Strasser *et al.*, 2010; Salvatori *et al.*, 2014; Shen *et al.*, 2016). To test PSI activity and the connectivity of the two photosystems of triggered *Dionaea* traps, kinetics of the normalized modulated reflection at 820 nm expressed by the MR/MR_0 ratio were recorded between 0 and 300 s following trap stimulation (Fig. 3 logarithmic time scale). In the literature, the P700/PC redox mechanism is described as follows. After the onset of actinic illumination, MR/MR_0 normally decreases (Salvatori *et al.*, 2014). This corresponds to an increase in the concentration of oxidized states of PSI reaction centres ($P700^+$) and plastocyanin (PC^+), until a transitory steady state is reached (minimal MR/MR_0) where oxidation and re-reduction rates are equal. This initial (fast) phase (from 0.7 to 20 ms) is followed by a slow phase where the increase of the MR/MR_0 ratio indicates $P700^+$ and PC^+ re-reduction, and the electron flow from PSII leads to an electron flow through PSI, when electrons arrive from PSII via intersystem electron carriers (Strasser *et al.*, 2010; Oukarroum *et al.*, 2016).

In the present study, modulated reflection was measured on open traps (Fig. 3, green symbols). Only a moderate decrease of the MR signal was detected in the first 20 ms after exposure to strong actinic light, indicating a very low increase of oxidized forms of PSI reaction centres and PC. Obviously, most of the P700 remained in the reduced state. Traps were mechanically triggered to close and MR was measured several times between 1 min and 24 h after trap closure (non-fed traps; Fig. 3A). Closed non-fed traps showed a slightly higher oxidation rate (expressed as lower MR/MR_0 values), with no significant changes within the first 20 min after trap closure compared with

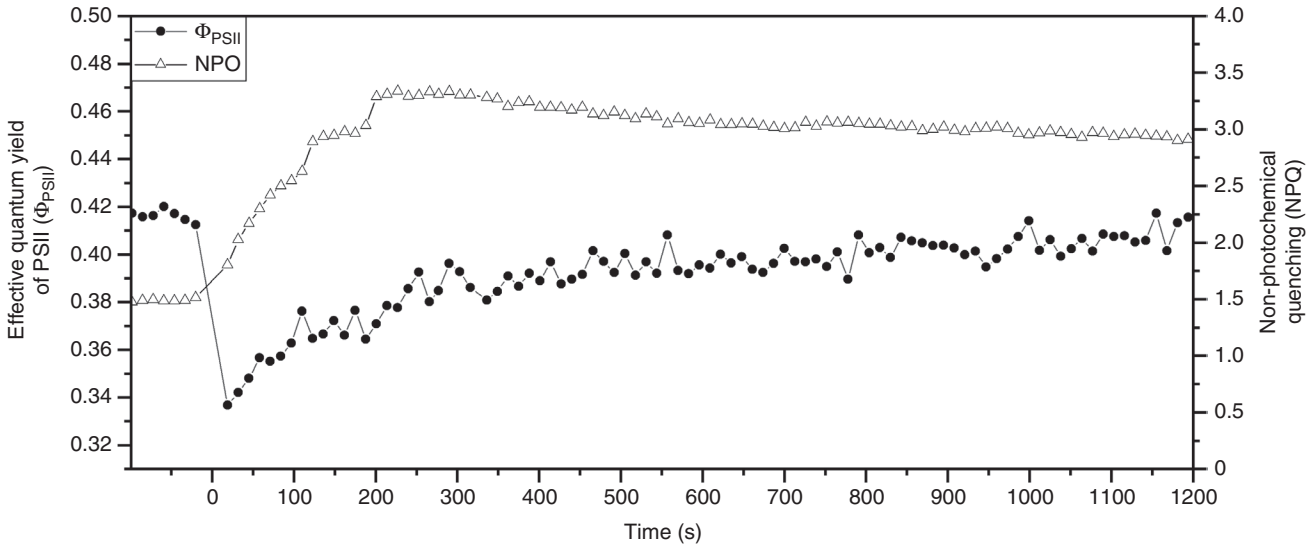

FIG. 2. Response of non-photochemical quenching (NPQ) and effective quantum yield (Φ_{PSII}) in *Dionaea muscipula* after stimulation of trigger hairs ($t = 0$) (trap temperature 25 °C, light intensity 150 µmol m^{-2} s^{-1} PAR, CO_2 concentration 400 µL L^{-1}, relative air humidity 65 %). Measurements were conducted using the PAM Fluorometer 3033-FL-Module of the gas exchange measuring system GFS-3000 (Walz) concurrently with net assimilation measurements (Fig. 1). Data shown are mean values based on five independent measurements.

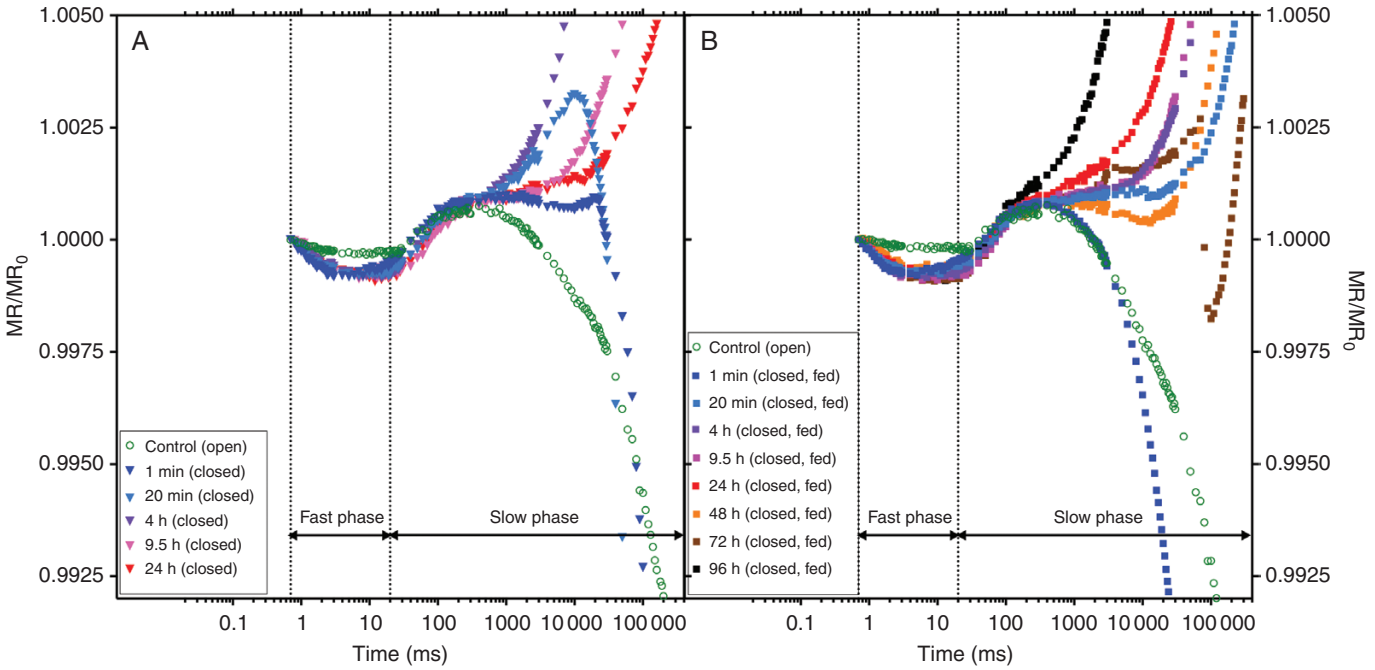

FIG. 3. Modulated reflection at 820 nm. Kinetics (induction curves) of modulated 820 nm reflection (MR) induced by a 300 s pulse of strong red actinic light (627 nm peak, 3500 µmol photons m^{-2} s^{-1}) in *Dionaea muscipula* traps dark-adapted for 20 min, measured with M-PEA2 and plotted on a logarithmic time scale from 0 to 300 s. The modulated reflection signals are expressed by the MR/MR_0 ratio, where MR_0 is the value at the onset of the actinic illumination (taken at 0.7 ms, the first reliable MR measurement). (A) MR/MR_0 ratio of traps mechanically triggered to close measured within a time period of 24 h after trap closing. Green circles: $t = 0$ open traps before triggering. Filled downwards triangles: dark blue $t = 1$ min, light blue $t = 20$ min, purple $t = 4$ h, pink $t = 9.5$ h, red $t = 24$ h after trap closing. (B) MR/MR_0 ratio of traps fed with insect powder and triggered mechanically to close, measured within a time period of 96 h after trap closing. Filled green circles: $t = 0$ open traps before triggering. Filled squares: dark blue $t = 1$ min, light blue $t = 20$ min, purple $t = 4$ h, pink $t = 9.5$ h, red $t = 24$ h, orange $t = 48$ h, brown $t = 72$ h and black $t = 96$ h. Data shown are mean values based on eight individual measurements.

open traps (Fig. 3A; Supplementary Data Fig. S1a). All non-fed traps of *Dionaea* re-opened within 24–48 h after closure. For another group of *Dionaea* plants, 10 mg of insect paste together with 25 µL of Gln was supplied as bait in addition to the mechanical stimulus. In contrast to non-fed traps, the modulated reflection patterns of fed traps were significantly different from open traps already 1 min after trap closure (Fig. 3B; Supplementary Data Fig. S1a). Traps remained closed beyond 24 h after mechanical stimulation (Fig. 3B) since they were able to hermetically seal the capture organ and build a 'green stomach', as described in a previous study (Böhm *et al.*, 2016).

In contrast to the transient initial (fast) phase (from 0.7 to 20 ms), after a transitory steady state was reached at about 20 ms, the kinetics of the normalized modulated reflection at 820 nm of non-fed traps showed a different pattern compared with the control during the slow phase (slow phase starts at t >20 ms) (Fig. 3A, B). Measurements of non-fed traps at 4 h (Fig. 3A, purple triangles), as well as at 9.5 and 24 h after closure (Fig. 3A, pink and red triangles, respectively), showed a steep increase of the modulated reflection signal (t >500 ms) compared with open traps (green circles), but also with closed traps measured 1 min and 20 min after closure (Fig. 3A). Apparently, the redox state of PC and P700 was shifted towards reduced states under actinic illumination. In fed traps, these shifts towards reduced states in the slow phase were observed already 20 min after closure (Fig. 3B, light blue filled squares), an indication of a different physiological response of fed traps compared with non-fed closed traps. These changes in the physiological behaviour within the redox state of PC and P700 upon stimulation point to a shift in ratios between linear and cyclic electron transport characterized by an enhanced cyclic electron transport (Walker *et al.*, 2014). Different physiological responses between fed and non-fed traps could be a result of nutrient and/or carbohydrate uptake from prey. This view is supported by measurements of N contents in tissues of *Dionaea* traps fed with amino acids that showed much higher N contents than in non-fed traps (Fasbender *et al.*, 2017).

The shape of modulated reflection curves measured at 820 nm in traps of *Dionaea* differed from measurements conducted with other species (e.g. Strasser *et al.*, 2010; Shen *et al.*, 2016; Zhang *et al.*, 2016), as well as results of our own measurements performed on different plant species [*Ipomoea batatas* (L.) LAM. and *Nicotiana tabacum* L.] grown under the same conditions as the *Dionaea* plants used for the experiments (Supplementary Data Fig. S2). During the fast phase (t <20 ms), a much more pronounced decrease of the signals was recorded with these species, indicating higher oxidation rates towards PC^+ and $P700^+$ compared with traps of *Dionaea* (Supplementary Data Fig. S2).

Prompt chlorophyll fluorescence

In parallel to measurements of the modulated reflection, prompt Chl fluorescence signals (PF) were recorded with the same instrument as for the modulated reflection (Fig. 4). Induction curves, normalized to the basal fluorescence F_0 of the

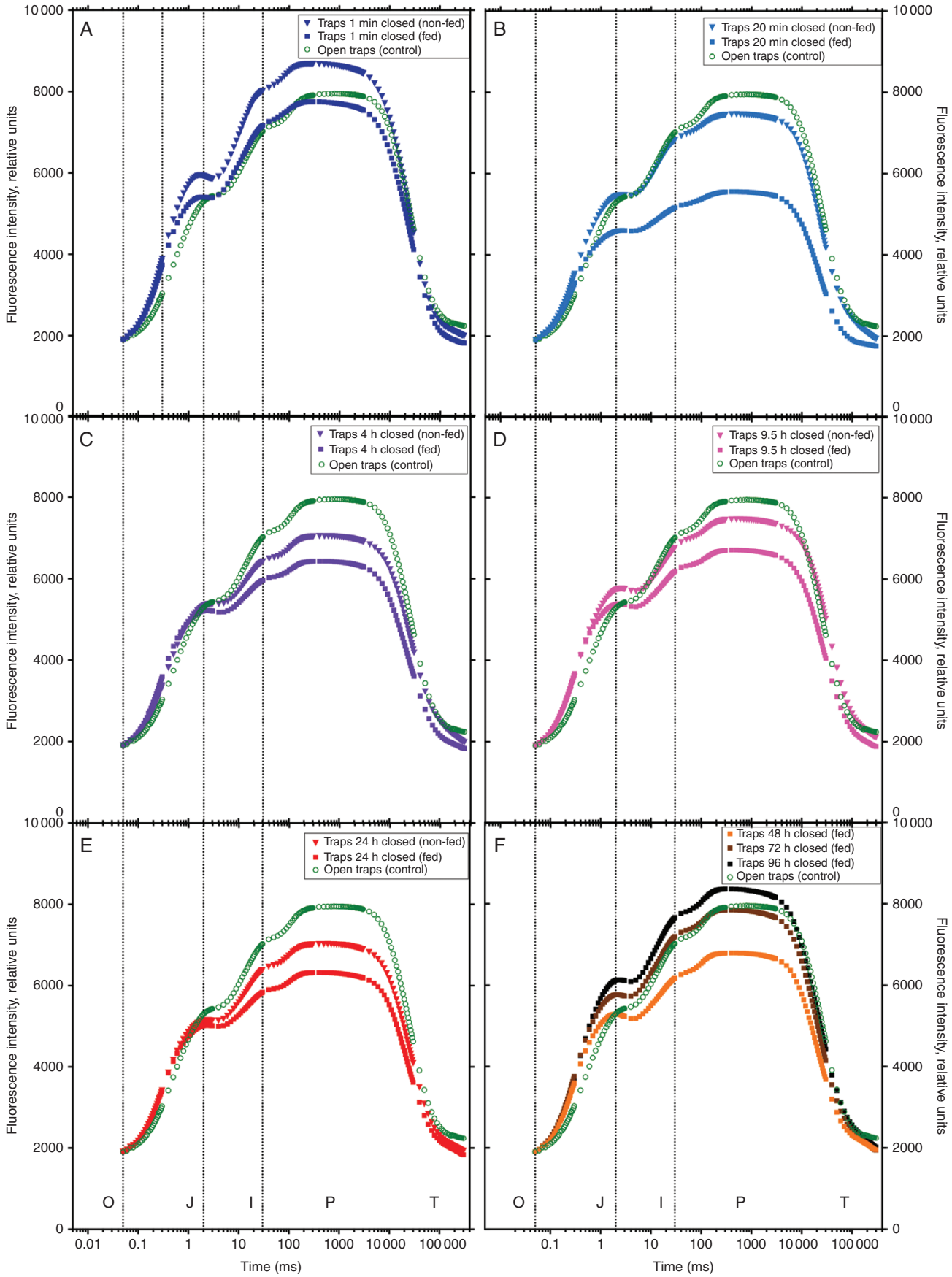
A
Traps 1 min closed (non-fed)
Traps 1 min closed (fed)
Open traps (control)
B
Traps 20 min closed (non-fed)
Traps 20 min closed (fed)
Open traps (control)
C
Traps 4 h closed (non-fed)
Traps 4 h closed (fed)
Open traps (control)
D
Traps 9.5 h closed (non-fed)
Traps 9.5 h closed (fed)
Open traps (control)
E
Traps 24 h closed (non-fed)
Traps 24 h closed (fed)
Open traps (control)
F
Traps 48 h closed (fed)
Traps 72 h closed (fed)
Traps 96 h closed (fed)
Open traps (control)
Fluorescence intensity, relative units
Time (ms)
O
J
I
P
T

dark-adapted sample, of measurements conducted 1 min after trap closure showed a similar shape for open and non-fed traps and no significant differences at the J-Step, I-Step and also at the peak (maximum) fluorescence F_P (Fig. 4A; Supplementary Data S1b–d). Twenty minutes after closure, the induction curves of non-fed traps were similar to those of open controls. In contrast to these findings, measurements performed with fed traps showed highly significant differences 20 min after closure at the intermediate step of fluorescence (I) and the peak of fluorescence (P), a time range of the PSII fluorescence kinetics, where plastocyanin and P700 are located, but not at the J-Step (Fig. 4B; Supplementary Data Fig. S1b–d). It is generally accepted that the first phase of the fluorescence transient (O–J) represents the photochemical processes within PSII, i.e. the gradual reduction of QA, the primary electron acceptor in PSII (e.g. Stirbet and Govindjee, 2012). Chl fluorescence signals (PF) measured on fed traps closed for 4 h were still significantly lower from I to P (Fig. 4C; Supplementary Data Fig. S1c–d). Fluorescence induction curves of fed traps closed for 9.5 h and longer showed no significant differences compared with open controls (Fig. 4D–F; Supplementary Data Fig. S1b–d). In contrast to traps fed with insect powder, no significant differences in Chl fluorescence induction curves were detected for non-fed closed traps compared with open controls (Fig. 4A–E).

Many photosynthetic processes influence the kinetics of the fast Chl *a* fluorescence rise from origin O to peak P (Stirbet *et al.*, 2018). Much information is available about the effect of different stressors on the fluorescence induction curves in plants, e.g. high light conditions (Lazár, 2006), high temperatures (Tóth *et al.*, 2007; Mathur *et al.*, 2011), low temperatures (Strauss *et al.*, 2007; Gururani *et al.*, 2015), drought (Goltsev *et al.*, 2012; Meng *et al.*, 2016), salt (Misra *et al.*, 2001), N deficiency (Cetner *et al.*, 2017; Zhao *et al.*, 2017), ozone (Cascio *et al.*, 2010) and heavy metals (Xue *et al.*, 2014). Despite the large number of publications, not much information is available about the Chl fluorescence induction of carnivorous plants. In two previous publications, fast fluorescence measurements were performed on *D. muscipula*. In contrast to the present study, measured on traps attached to the plants (Fig. 4), only small effects on the fast Chl *a* fluorescence transient were observed for detached traps (Pavlovič *et al.*, 2011). A second publication on attached traps was focused on different excitation light intensities, and measurements right after trap closure recorded only small differences in the I–P phase. Effects in the time range longer than seconds after trap closure were not measured (Vredenberg and Pavlovič, 2013). According to publications on non-carnivorous plants, PSI activity is related to the I–P phase (between 30 ms and 1 s) of the fluorescence kinetics, parallels the reduction of PC^+ and $P700^+$ (Schansker *et al.*, 2005), indicates the rate of reduction of ferredoxin (Cascio *et al.*, 2010) and is considered to constitute a measure for the size of PSI electron acceptors (Tsimilli-Michael and Strasser, 2008; Živčák *et al.*, 2014). The present results show clear differences between 2 ms (J) and 30 ms (I) already 20 min after trap closure, but only for closed traps fed with insect powder. Closed traps without insect powder showed no difference from open traps at all. The J–I phase is related to the plastoquinone pool redox state (Tóth *et al.*, 2007). Since there are large effects of trap closure in this phase, in fed traps, this result indicates cyclic electron transport in which plastoquinone is involved (Allen, 2004).

ATP content of midribs and traps

Cyclic electron flow around PSI occurs to balance the production and consumption of ATP, which is needed in particular to meet the changing energy demands for assimilating N (Walker *et al.* 2014). Cyclic electron transport in photosynthesis is required when the total demand for ATP exceeds the demand for ATP in basic CO_2 fixation reactions. Differences between the supply of ATP from linear electron transport and an increased demand could be balanced via cyclic electron flow (Kramer and Evans, 2011; Walker *et al.*, 2014; Yamori *et al.*, 2016).

Therefore, we analysed the ATP content in whole traps and in midribs that have an exceptional ATP demand in connection with trap closure, 'green stomach' formation, hydrolase secretion and prey digestion. Immediately after trap closure, ATP contents of non-fed midribs decreased by 23 % (Fig. 5), which is similar to the 31 % decline previously observed (Jaffe, 1973). ATP content transiently further decreased up to 73 % after 24 h compared with open control traps; thereafter, the ATP level of the midribs increased steadily in the subsequent 48 h. At the whole-trap level, no significant changes of ATP contents after trap closure of non-fed traps were observed (Fig. 6). Previously, a decline of 29 % was observed for ATP contents of whole traps (Williams and Bennett, 1982). Similar to non-fed traps, ATP contents of midribs of fed traps decreased in the first 4 h after trap closure (Fig. 5). In contrast, ATP contents increased significantly between 4 and 24 h and decreased slowly afterwards. No changes of ATP contents of the whole trap were observed in fed traps after trap closure, similarly to non-fed traps (Fig. 6).

ATP contents were not significantly changed during closure in fed and non-fed traps in the first 9.5 h, which illustrates that ATP homeostasis was achieved at the whole-trap level (Fig. 6) and tissue analysis is required. However, in midribs of both fed and non-fed traps, ATP contents decreased significantly in the first 30 s after trap closure and stayed at a low level for the following 4 h, which indicates that already in the early phase after triggering and trap closure, large amounts of ATP/energy are required. The midrib is a vascular-rich site that channels nutrients out of the trap. Early ATP consumption indicates that transporters are quickly expressed and upregulated for the future export of nutrients. Early expression and upregulation of

FIG. 4. Prompt Chl *a* fluorescence. Prompt fluorescence transients of *Dionaea muscipula* traps dark-adapted for 20 min and transients, measured with M-PEA induced by red actinic light of 3500 µmol photons m^{-2} s^{-1} and plotted on a logarithmic time scale from 0 to 300 s normalized at t = 50 µs (F_0); the steps O ('origin' at 50 µs), J (at 2 ms) and I (at 30 ms), peak P (between 200 ms and 1 s) and 'terminal steady state' T (at about 300 s) are marked. (A–E) Green open circles, open traps at t = 0; downwards filled triangles, closed traps mechanically triggered to close; filled squares, traps fed with insect powder and mechanically triggered to close; at different times after trap closure. Time: (A) dark blue symbols, t = 1 min; (B) light blue symbols, t = 20 min; (C) purple symbols, t = 4 h; (D) pink symbols, t = 9.5 h; (E) red symbols, t = 24 h. In (F) closed traps fed with insect powder at t = 48 h (orange filled squares); t = 72 h (brown filled squares) and 96 h (black filled squares). Data shown are mean values based on eight individual measurements.

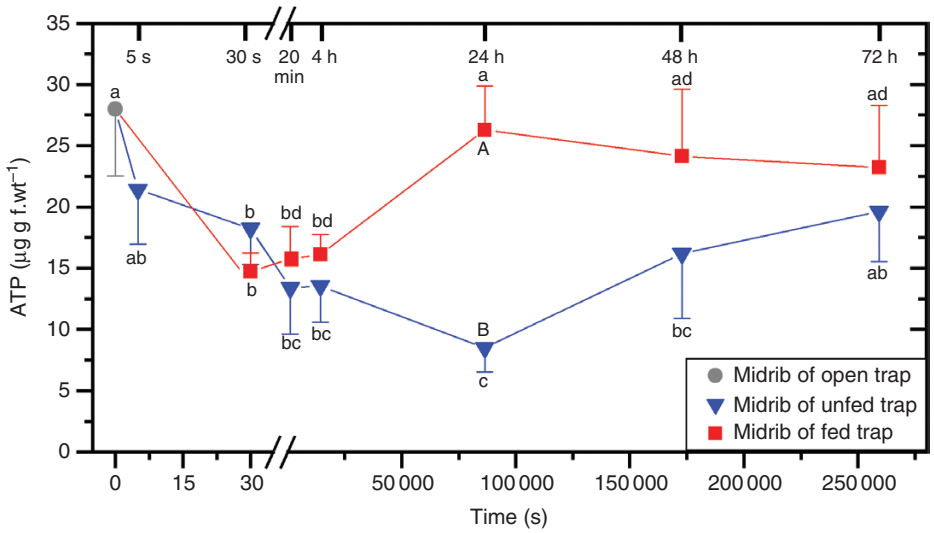

FIG. 5. ATP values of midribs in *Dionaea muscipula* traps in unfed open control traps, unfed mechanically triggered traps and fed mechanically triggered traps. Midribs were cut out of snap-frozen *Dionaea* traps with a scalpel before they were homogenized into powder with a mortar and pestle and ATP values were determined using an ATP assay kit. Significant differences between different time points within one treatment are indicated by lower case letters and differences between both treatments at the same time point are indicated with upper case letters. Data shown are mean values (± s.d.) based on five independent measurements.

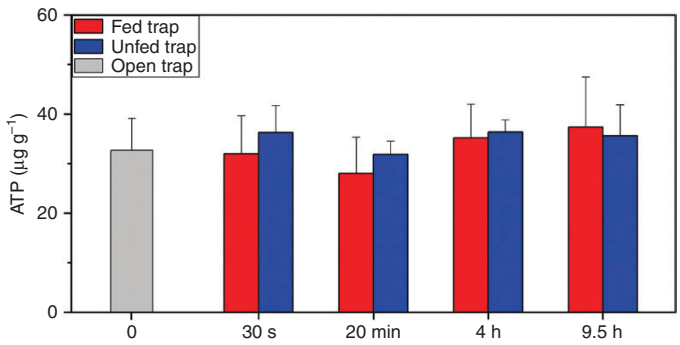

FIG. 6. ATP values of traps in *Dionaea muscipula* in unfed open control traps, unfed mechanically triggered traps and fed mechanically triggered traps. Data shown are mean values (± s.d.) based on five independent measurements. Significant differences were not observed.

transporters in glands were already observed for ammonium (Scherzer *et al.*, 2013), potassium (Scherzer *et al.*, 2015) and sodium (Böhm *et al.*, 2016). The upregulation of transporters is probably also the reason for further ATP consumption in midribs of non-fed traps 24 h after trap closure. All non-fed traps started to re-open 24 h after closure. Although additional ATP is likely to be needed during re-opening of traps, ATP values of the midribs were rising during the next 48 h, making traps ready for a new approach to capture prey.

In a previous labelling study, high-resolution isotope analyses of emitted CO_2 by isotope ratio infrared spectroscopy showed the respiratory use of prey-derived carbon approx. 5 h after trap closure (Fasbender *et al.*, 2017). This respiratory use coincides with the increase in midrib ATP levels beyond 4 h after trap closure, indicating respiratory ATP production from prey-derived carbon. However, finally ATP production from prey resources inside the traps may compete with the export of prey-derived intermediates to other plant organs. This export will consume energy and may be responsible for the decline of the ATP level in fed traps 24 h after closure.

Conclusions

The present results indicate that upon prey capture by *D. muscipula* snap traps, a switch from linear to cyclic electron transport mediates partial ATP homeostasis despite high ATP consumption for processes related to trap closure, 'green stomach' formation, hydrolase secretion and prey digestion. ATP from prey-derived sources seems to contribute to the ATP content of the traps beyond 4 h of prey capture. Approximately 24 h after prey capture, export of prey-derived resources to other plant organs may become preferential and causes a decline in ATP contents. A detailed resolution of continuing metabolic processes, such as transport of prey metabolites, their distribution and early degradation inside the traps, requires the development of tissue-specific, isotope ratio mass spectrometry-coupled gas chromatography–mass spectroscopy analyses in future studies.

SUPPLEMENTARY DATA

Supplementary data are available online at https://academic.oup.com/aob and consist of the following.

Figure S1: variation of replicates and levels of significance in modulated reflection and prompt chlorophyll fluorescence.

Figure S2: modulated 820 nm reflection in *Ipomoea batatas* (L.) LAM. and *Nicotiana tabacum* L.

FUNDING

The authors extend their appreciation to the Deanship of Scientific Research at King Saud University, Saudi Arabia, for funding this work through research group RG-1435-018.

ACKNOWLEDGEMENTS

We thank Mr Rod Humby, managing director of Hansatech Instruments Ltd, King's Lynn, UK, for providing the M-PEA,

used for chlorophyll fluorescence measurements and measurements of modulated reflection.

LITERATURE CITED

Adamec L. 1997. Mineral nutrition of carnivorous plants: a review. *Botanical Review* **63:** 273–299.

Adlassnig W, Peroutka M, Lambers H, Lichtscheidl IK. 2005. The roots of carnivorous plants. *Plant and Soil* **274:** 127–140.

Allen JF. 2004. Chloroplast redox poise and signaling. In: Lennarz W, Lane M, eds. *Encyclopedia of biological chemistry*, Vol. **1**. Elsevier **1:** 438–445.

Bemm F, Becker D, Larisch C, *et al.* 2016. Venus flytrap carnivorous lifestyle builds on herbivore defense strategies. *Genome Research* **26:** 812–825.

Benzing DH. 2000. *Bromeliaceae: profile of an adaptive radiation*. Cambridge: Cambridge University Press.

Benzing DH, Henderson K, Kessel B, Sulak J. 1976. The absorptive capacities of bromeliad trichomes. *American Journal of Botany* **63:** 1009–1014.

Böhm J, Scherzer S, Shabala S, *et al.* 2016. Venus flytrap HKT1-type channel provides for prey sodium uptake into carnivorous plant without conflicting with electrical excitability. *Molecular Plant* **9:** 428–436.

Brewer JS, Baker DJ, Nero AS, Patterson AL, Roberts RS, Turner LM. 2011. Carnivory in plants as a beneficial trait in wetlands. *Aquatic Botany* **94:** 62–70.

Bruzzese BM, Bowler R, Massicotte HB, Fredeen AL. 2010. Photosynthetic light response in three carnivorous plant species: *Drosera rotundifolia*, *D. capensis* and *Sarracenia leucophylla*. *Photosynthetica* **48:** 103–109.

Cascio C, Schaub M, Novak K, Desotgiu R, Bussotti F, Strasser RJ. 2010. Foliar responses to ozone of *Fagus sylvatica* L. seedlings grown in shaded and in full sunlight conditions. *Environmental and Experimental Botany* **68:** 188–197.

Cetner MD, Kalaji HM, Goltsev V, *et al.* 2017. Effects of nitrogen-deficiency on efficiency of light-harvesting apparatus in radish. *Plant Physiology and Biochemistry* **119:** 81–92.

Chen S, Yang J, Zhang M, Strasser RJ, Qiang S. 2016. Classification and characteristics of heat tolerance in *Ageratina adenophora* populations using fast chlorophyll a fluorescence rise O–J–I–P. *Environmental and Experimental Botany* **122:** 126–140.

Ellison AM. 2006. Nutrient limitation and stoichiometry of carnivorous plants. *Plant Biology* **8:** 740–747.

Ellison AM, Adamec L. 2011. Ecophysiological traits of terrestrial and aquatic carnivorous plants: are the costs and benefits the same? *Oikos* **120:** 1721–1731.

Escalante-Pérez M, Scherzer S, Al-Rasheid KAS, Döttinger C, Neher E, Hedrich R. 2014. Mechano-stimulation triggers turgor changes associated with trap closure in the Darwin plant *Dionaea muscipula*. *Molecular Plant* **7:** 744–746.

Escher P, Eiblmeier M, Hetzger I, Rennenberg H. 2004*a*. Spatial and seasonal variation in amino compounds in the xylem sap of a mistletoe (*Viscum album*) and its hosts (*Populus* spp. and *Abies alba*). *Tree Physiology* **24:** 639–650.

Escher P, Eiblmeier M, Hetzger I, Rennenberg H. 2004*b*. Seasonal and spatial variation of carbohydrates in mistletoes (*Viscum album*) and the xylem sap of its hosts (*Populus* × *euamericana* and *Abies alba*). *Physiologia Plantarum* **120:** 212–219.

Fasbender L, Maurer D, Kreuzwieser J, *et al.* 2017. The carnivorous Venus flytrap uses prey-derived amino acid carbon to fuel respiration. *New Phytologist* **214:** 597–606.

Gao P, Loeffler TS, Honsel A, *et al.* 2015. Integration of trap- and root-derived nitrogen nutrition of carnivorous *Dionaea muscipula*. *New Phytologist* **205:** 1320–1329.

Goltsev V, Zaharieva I, Chernev P, *et al.* 2012. Drought-induced modifications of photosynthetic electron transport in intact leaves: analysis and use of neural networks as a tool for a rapid non-invasive estimation. *Biochimica et Biophysica Acta* **1817:** 1490–1498.

Graham SW, Lam VKY, Merckx VSFT. 2017. Plastomes on the edge: the evolutionary breakdown of mycoheterotroph plastid genomes. *New Phytologist* **214:** 48–55.

Gururani MA, Venkatesh J, Ganesan M, *et al.* 2015. In vivo assessment of cold tolerance through chlorophyll-a fluorescence in transgenic zoysiagrass expressing mutant phytochrome A. *PLoS One* **10:** e0127200. doi: 10.1371/journal.pone.0127200.

Hedrich R, Neher E. 2018. Venus flytrap: how an excitable, carnivorous plant works. *Trends in Plant Science* **23:** 220–234.

Jaffe MJ. 1973. The role of ATP in mechanically stimulated rapid closure of the Venus's flytrap. *Plant Physiology* **51:** 17–18.

Klughammer C, Schreiber U. 1998. Measuring P700 absorbance changes in the near infrared spectral region with a dual wavelength pulse modulation system. In: Garab G, eds. *Photosynthesis: mechanisms and effects*. Dordrecht: Springer, 4357–4360.

Kramer DM, Evans JR. 2011. The importance of energy balance in improving photosynthetic productivity. *Plant Physiology* **155:** 70–78.

Kruse J, Gao P, Honsel A, *et al.* 2014. Strategy of nitrogen acquisition and utilization by carnivorous *Dionaea muscipula*. *Oecologia* **174:** 839–851.

Kruse J, Gao P, Eibelmeier M, Alfarraj S, Rennenberg H. 2017. Dynamics of amino acid redistribution in the carnivorous Venus flytrap (*Dionaea muscipula*) after digestion of 13 C/15 N-labelled prey. *Plant Biology* **19:** 886–895.

Lasso E, Ackerman JD. 2013. Nutrient limitation restricts growth and reproductive output in a tropical montane cloud forest bromeliad: findings from a long-term forest fertilization experiment. *Oecologia* **171:** 165–174.

Lazár D. 2006. The polyphasic chlorophyll a fluorescence rise measured under high intensity of exciting light. *Functional Plant Biology* **33:** 9–30.

Li FJ, Xu ZS, Soo ADS, Lun ZR, He CY. 2017. ATP-driven and AMPK-independent autophagy in an early branching eukaryotic parasite. *Autophagy* **13:** 715–729.

Mathur S, Allakhverdiev SI, Jajoo A. 2011. Analysis of high temperature stress on the dynamics of antenna size and reducing side heterogeneity of Photosystem II in wheat leaves (*Triticum aestivum*). *Biochimica et Biophysica Acta* **1807:** 22–29.

Meng L-L, Song J-F, Wen J, Zhang J, Wei J-H. 2016. Effects of drought stress on fluorescence characteristics of photosystem II in leaves of *Plectranthus scutellarioides*. *Photosynthetica* **54:** 414–421.

Misra AN, Srivastava A, Strasser RJ. 2001. Utilization of fast chlorophyll a fluorescence technique in assessing the salt/ion sensitivity of mung bean and Brassica seedlings. *Journal of Plant Physiology* **158:** 1173–1181.

Nevill PG, Howell KA, Cross AT, *et al.* 2019. Plastome-wide rearrangements and gene losses in carnivorous droseraceae. *Genome Biology and Evolution* **11:** 472–485.

Nishi AH, Vasconcellos-Neto J, Romero GQ. 2013. The role of multiple partners in a digestive mutualism with a protocarnivorous plant. *Annals of Botany* **111:** 143–150.

Oukarroum A, El Madidi S, Strasser RJ. 2016. Differential heat sensitivity index in barley cultivars (*Hordeum vulgare L.*) monitored by chlorophyll a fluorescence OKJIP. *Plant Physiology and Biochemistry* **105:** 102–108.

Pavlovič A, Demko V, Hudák J. 2010. Trap closure and prey retention in Venus flytrap (*Dionaea muscipula*) temporarily reduces photosynthesis and stimulates respiration. *Annals of Botany* **105:** 37–44.

Pavlovič A, Slováková L, Pandolfi C, Mancuso S. 2011. On the mechanism underlying photosynthetic limitation upon trigger hair irritation in the carnivorous plant Venus flytrap (*Dionaea muscipula* Ellis). *Journal of Experimental Botany* **62:** 1991–2000.

Petersen G, Cuenca A, Seberg O. 2015. Plastome evolution in hemiparasitic mistletoes. *Genome Biology and Evolution* **7:** 2520–2532.

Roberts PR, Oosting HJ. 1958. Responses of Venus fly trap (*Dionaea muscipula*) to factors involved in its endemism. *Ecological Monographs* **28:** 193–218.

Salvatori E, Fusaro L, Gottardini E, *et al.* 2014. Plant stress analysis: application of prompt, delayed chlorophyll fluorescence and 820nm modulated reflectance. Insights from independent experiments. *Plant Physiology and Biochemistry* **85:** 105–113.

Schansker G, Srivastava A, Govindjee, Strasser RJ. 2003. Characterization of the 820-nm transmission signal paralleling the chlorophyll a fluorescence rise (OJIP) in pea leaves. *Functional Plant Biology* **30:** 785–796.

Schansker G, Tóth SZ, Strasser RJ. 2005. Methylviologen and dibromothymoquinone treatments of pea leaves reveal the role of photosystem I in the Chl a fluorescence rise OJIP. *Biochimica et Biophysica Acta* **1706:** 250–261.

Scherzer S, Krol E, Kreuzer I, *et al.* 2013. The *Dionaea muscipula* ammonium channel DmAMT1 provides NH_4^+ uptake associated with venus flytrap's prey digestion. *Current Biology* **23:** 1649–1657.

Scherzer S, Böhm J, Krol E, *et al.* 2015. Calcium sensor kinase activates potassium uptake systems in gland cells of Venus flytraps. *Proceedings of the National Academy of Sciences, USA* **112:** 7309–7314.

Scherzer S, Shabala L, Hedrich B, *et al.* 2017. Insect haptoelectrical stimulation of Venus flytrap triggers exocytosis in gland cells. *Proceedings of the National Academy of Sciences, USA* **114:** 4822–4827.

Schreiber U, Klughammer C, Neubauer C. 1988. Measuring P700 absorbance changes around 830 nm with a new type of pulse modulation system. *Zeitschrift für Naturforschung C* **43:** 686–698.

Schneider CA, Rasband WS, Eliceiri KW. 2012. NIH Image to ImageJ: 25 years of image analysis. *Nature Methods* **9:** 671–675.

Schulze W, Schulze ED, Schulze I, Oren R. 2001. Quantification of insect nitrogen utilization by the venus fly trap *Dionaea muscipula* catching prey with highly variable isotope signatures. *Journal of Experimental Botany* **52:** 1041–1049.

Shen W, Ye L, Ma J, *et al.* 2016. The existence of C4-bundle-sheath-like photosynthesis in the mid-vein of C3 rice. *Rice* **9:** 20. doi: 10.1186/s12284-016-0094-5.

Shin HW, Lee NS. 2018. Understanding plastome evolution in hemiparasitic santalales: complete chloroplast genomes of three species, *Dendrotrophe varians*, *Helixanthera parasitica*, and *Macrosolen cochinchinensis*. *PLoS One* **13:** e0200293. doi: 10.1371/journal.pone.0200293.

Smith CM. 1931. Development of *Dionaea muscipula*. II. Germination of seed and development of seedling to maturity. *Botanical Gazette* **91:** 377–394.

Stirbet A, Govindjee. **2012.** Chlorophyll a fluorescence induction: a personal perspective of the thermal phase, the J–I–P rise. *Photosynthesis Research* **113:** 15–61.

Stirbet A, Lazár D, Kromdijk J, Govindjee. **2018.** Chlorophyll a fluorescence induction: can just a one-second measurement be used to quantify abiotic stress responses? *Photosynthetica* **56:** 86–104.

Strasser RJ, Tsimilli-Michael M, Qiang S, Goltsev V. 2010. Simultaneous *in vivo* recording of prompt and delayed fluorescence and 820-nm reflection changes during drying and after rehydration of the resurrection plant *Haberlea rhodopensis*. *Biochimica et Biophysica Acta* **1797:** 1313–1326.

Strauss AJ, Krüger GHJ, Strasser RJ, Van Heerden PDR. 2007. The role of low soil temperature in the inhibition of growth and PSII function during dark chilling in soybean genotypes of contrasting tolerance. *Physiologia Plantarum* **131:** 89–105.

Takahashi CA, Mercier H. 2011. Nitrogen metabolism in leaves of a tank epiphytic bromeliad: characterization of a spatial and functional division. *Journal of Plant Physiology* **168:** 1208–1216.

Tóth SZ, Schansker G, Garab G, Strasser RJ. 2007. Photosynthetic electron transport activity in heat-treated barley leaves: the role of internal alternative electron donors to photosystem II. *Biochimica et Biophysica Acta* **1767:** 295–305.

Tsimilli-Michael M, Strasser RJ. 2008. In vivo assessment of stress impact on plant's vitality: applications in detecting and evaluating the beneficial role of mycorrhization on host plants. In: Varma A, ed. *Mycorrhiza*. Berlin Heidelberg: Springer, 679–703.

Volkov AG, Adesina T, Markin VS, Jovanov E. 2008. Kinetics and mechanism of *Dionaea muscipula* trap closing. *Plant Physiology* **146:** 694–702.

Volkov AG, Murphy VA, Clemmons JI, Curley MJ, Markin VS. 2012. Energetics and forces of the *Dionaea muscipula* trap closing. *Journal of Plant Physiology* **169:** 55–64.

Vredenberg W, Pavlovič A. 2013. Chlorophyll a fluorescence induction (Kautsky curve) in a Venus flytrap (*Dionaea muscipula*) leaf after mechanical trigger hair irritation. *Journal of Plant Physiology* **170:** 242–250.

Walker BJ, Strand DD, Kramer DM, Cousins AB. 2014. The response of cyclic electron flow around photosystem I to changes in photorespiration and nitrate assimilation. *Plant Physiology* **165:** 453–462.

Wicke S, Schäferhoff B, Depamphilis CW, Müller KF. 2014. Disproportional plastome-wide increase of substitution rates and relaxed purifying selection in genes of carnivorous lentibulariaceae. *Molecular Biology and Evolution* **31:** 529–545.

Williams SE, Bennett AB. 1982. Leaf closure in the venus flytrap: an acid growth response. *Science* **218**: 1120–1122.

Xue Z, Gao H, Zhao S. 2014. Effects of cadmium on the photosynthetic activity in mature and young leaves of soybean plants. *Environmental Science and Pollution Research* **21:** 4656–4664.

Yang N-C, Ho W-M, Chen Y-H, Hu M-L. 2002. A convenient one-step extraction of cellular ATP using boiling water for the luciferin-luciferase assay of ATP. *Analytical Biochemistry* **306:** 323–327.

Yamori W, Makino A, Shikanai T. 2016. A physiological role of cyclic electron transport around photosystem I in sustaining photosynthesis under fluctuating light in rice. *Scientific Reports* **6:** 20147. doi: 10.1038/srep20147.

Zhang Z, Qiao M, Li D, Yin H, Liu Q. 2016. Do warming-induced changes in quantity and stoichiometry of root exudation promote soil N transformations via stimulation of soil nitrifiers, denitrifiers and ammonifiers? *European Journal of Soil Biology* **74:** 60–68.

Zhao LS, Li K, Wang QM, *et al.* 2017. Nitrogen starvation impacts the photosynthetic performance of *Porphyridium cruentum* as revealed by chlorophyll a fluorescence. *Scientific Reports* **7:** 8542. doi: 10.1038/s41598-017-08428-6.

Živčák M, Olšovská K, Slamka P, *et al.* 2014. Application of chlorophyll fluorescence performance indices to assess the wheat photosynthetic functions influenced by nitrogen deficiency. *Plant, Soil and Environment* **60:** 210–215.